Food Chemistry: X 24 (2024) 101909

Contents lists available at ScienceDirect

Food Chemistry: X

journal homepage: www.sciencedirect.com/journal/food-chemistry-x

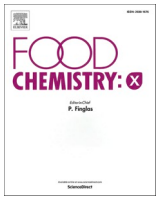

Comparison and chemometrics analysis of phenolic compounds and mineral elements in Artemisia Argyi Folium from different geographical origins

Lifei Hu [a,b,c], Fengxiao Zhu [a], Yifan Wang [a], Tao Wu [b,c], Xin Wu [b,c], Zhian Huang [b], Daihua Sun [c], Mingxing Liu [a,*]

[a] Cooperative Innovation Center of Industrial Fermentation (Ministry of Education & Hubei Province), National "111" Center for Cellular Regulation and Molecular Pharmaceutics, Key Laboratory of Fermentation Engineering (Ministry of Education), Hubei Key Laboratory of Industrial Microbiology, School of Life and Health Sciences, Hubei University of Technology, Wuhan 430068, China
[b] Hubei Key Lab of Quality and Safety of Traditional Chinese Medicine & Health Food, Huangshi 435100, China
[c] Hubei Provincial Engineering Technology Research Center of Traditional Chinese Medicine Formula Granules, Huangshi 435100, China

ARTICLE INFO

Keywords:
Artemisia Argyi Folium
Phenolic compounds
Mineral elements
Geographical origin
Chemometrics

ABSTRACT

The quality of Artemisia Argyi Folium (AAF), a traditional Chinese food ingredient, is intrinsically linked to its geographical origin, which this study explores through phenolic compounds and mineral elements. The contents of 17 phenols and 18 minerals differed significantly between geographically distinct samples according to UHPLC and ICP-MS, respectively. Chemometrics indicated that a supervised model, orthogonal partial least squares discriminant analysis (OPLS-DA), outperformed unsupervised methods at classifying AAF samples by their origins. Phenols were more effective at distinguishing samples from seven provinces, while minerals were adept at differentiating samples from the Dabie Mountain region (three provinces) and those from four other provinces. Six phenols and 10 minerals were important variables for discrimination. Complex correlations were observed between the contents of various phenols and minerals in AAF, with minerals possibly affecting the accumulation of phenols. This study provides an approach for distinguishing geographically distinct AAF samples and determining their geographical origins.

1. Introduction

Artemisia argyi Lévl. et Vant. is an edible and medicinal plant primarily distributed in China, Korea, Mongolia, and Japan. (Chang et al., 2021; Z. C. Wang et al., 2023). Artemisia Argyi Folium (AAF), which is commonly consumed as a traditional food ingredient, is used to prepare Chinese dishes such as qingtuan and dumplings (Cui et al., 2022; X. W. Song et al., 2019). AAF is composed of varied chemical constituents, including essential oils (Liu et al., 2021), flavonoids, phenolic acids (Li et al., 2019; W. Wu, Xiang, & He, 2021), terpenoids, and sterols (Zhan et al., 2022), which show antioxidant, hypoglycemic (Xiao et al., 2019), antimicrobial (H. B. Wang et al., 2020), anti-inflammatory (Chen et al., 2022), antitumor (Su et al., 2022), neuroprotective (L. K. Wu et al., 2022), and antiviral activities (X. W. Zhang et al., 2018).

The composition of food products is intricately linked to their provenance, and the variety and concentration of nutrients they contain are affected by crop soil quality, temperature, and other agricultural conditions (Jeong et al., 2023; Oliveira et al., 2019; Pacholczyk-Sienicka et al., 2024). Many different techniques have been proposed to determine the botanical and geographical origins of produce. Chemometrics combined with multi-component and multi-element analyses has proven efficacious when applied to diverse animal and plant products, such as honey, ginger, paprika, sesame, thyme, pork, and bovine bone (Campmajó et al., 2021; Qi et al., 2021; Wu, Xiang, & He, 2021; Wu, Zhao, et al., 2021; Yu et al., 2023).

A. argyi is cultivated in many regions of China, but Hubei Province is considered to provide one of the best sources of this plant's leaves (Liu et al., 2021). The quality and price of AAF from *A. argyi* plants of different geographical origins vary, but it is difficult to distinguish its origin by appearance only, leading to confusion about its provenance and limiting its commercial value. Hence, there is a need to develop a method of distinguishing AAF samples based on their components.

* Corresponding author.
E-mail address: lmxing@hbut.edu.cn (M. Liu).

https://doi.org/10.1016/j.fochx.2024.101909
Received 3 September 2024; Received in revised form 15 October 2024; Accepted 16 October 2024
Available online 18 October 2024

Phenolic compounds, such as phenolic acids and flavonoids, have demonstrated potential as pharmacological components of AAF (Li et al., 2019). Current research using phenolic compounds for fingerprint and quantitative analysis of non-volatile components of AAF still faces challenges such as long chromatographic separation times and poor separation of certain components(Chang et al., 2021; D. Zhang, Yao, et al., 2021). For example, cynarine and isochlorogenic acid A cannot be separated effectively. The method for quantitatively analyzing multi-index phenolic compounds requires further development. Alternatively, multi-isotopic and elemental signatures have proven to be effective for tracing the origins of foodstuffs. In contrast to stable isotope analysis, mineral element analysis has the advantages of rapidity, cost-effectiveness, and broad applicability (Nie et al., 2023; Qi et al., 2021). Moreover, chemometric methods can be utilized to analyze the phenolic compounds and mineral elements in AAF, enabling an examination and comparison of these components to trace the origins of AAF samples.

In this investigation, a comprehensive collection comprising 100 samples of AAF from *A. argyi* plants grown in seven provinces of China was amassed. Quantitative determination and comparison of 17 phenolic compounds (9 phenolic acids and 8 flavonoids) and 18 mineral elements from these samples was conducted. The components of the AAF samples were characterized using ultra-high performance liquid chromatography (UHPLC) with inductively coupled plasma mass spectrometry (ICP-MS) and chemometric techniques. Chemometrics, including hierarchical cluster analysis (HCA), principal component analysis (PCA), orthogonal partial least squares discriminant analysis (OPLS-DA), and Pearson's correlation analysis, were employed to analyze correlations between the components and classify AAF samples from various geographical origins.

The results indicated that the geographical origins of the samples could be distinguished by chemometric analysis of their contents of phenolic compounds and mineral elements, as these components were easy to classify and differentiate. This work contributes to a deeper and more comprehensive understanding of the characteristics of phenolic substances and mineral elements in AAF from plants of different geographical origins. The findings may also be used as a reference for AAF origin traceability analysis.

2. Material and methods

2.1. Reagents and standards

UHPLC-grade acetonitrile and formic acid were supplied by Fisher Chemical™ (Pittsburgh, PA, USA), and nitric acid and hydrochloric acid were obtained from Merck (Darmstadt, Germany). We sourced 95 % ethanol from Sinopharm Chemical Reagent Co., Ltd. (Shanghai, China). A range of reference compounds was obtained from the National Institute for Food and Drug Control (Beijing, China), including chlorogenic acid, caffeic acid, schaftoside, isochlorogenic acid C, apigenin, vitexicarpin, and isoquercitrin. Additional compounds such as neochlorogenic acid, isochlorogenic acid B, isochlorogenic acid A, hispidulin, and cynarine were purchased from Chengdu Desite Biological Technology Co., Ltd. (Chengdu, China). Jaceosidin and eupatilin were acquired from Sinco Pharmachem Inc. (Delaware, USA). Cryptochlorogenic acid was provided by Chengdu Must Biological Technology Co., Ltd. (Chengdu, China), and 3,4,5-tricaffeoylquinic acid was sourced from Wuhan ChemFaces Biochemical Co., Ltd. (Wuhan, China). The compound 5,7,3′-trihydroxy-6,4′,5′-trimethoxyflavone was secured from Shanghai Hongyong Biotechnology Co., Ltd. (Shanghai, China). The National Institute of Metrology (Beijing, China) provided the elemental standards. Purified water was obtained *via* an ELGA LabWater PURELAB Classic system (ELGA LabWater, UK) and underwent filtration using a 0.22 μm nylon membrane.

2.2. Plant materials

One hundred dried AAF samples were supplied by Jing Brand Chizhengtang Pharmaceutical Co., Ltd. (Huangshi, China). All samples were composed of dried leaves of *Artemisia argyi* Lévl. et Vant. The samples originated from *A. argyi* plants grown in Hubei Province (HUB, $n = 30$), Henan Province (HN, $n = 20$), Anhui Province (AH, $n = 10$), Jiangxi Province (JX, n = 10), Guizhou Province (GZ, n = 10), Hebei Province (HEB, n = 10), and Liaoning Province (LN, n = 10) in China (Fig. 1). All voucher specimens were taxonomically identified by Prof. Daihua Sun (Hubei Provincial Engineering Technology Research Center of Traditional Chinese Medicine Formula Granules, Huangshi, China). Before analysis, the samples were pulverized into a powder and screened using 50-mesh sieves (355 μm ± 13 μm) to ensure their suitability for the experiments. The samples were collected in June 2023.

2.3. Sample preparation

2.3.1. Preparation for UHPLC analysis

Precisely weighed quantities of 0.2 g of each powdered sample were placed into 50 mL conical flasks equipped with stoppers. Subsequently, 20 mL of 50 % ethanol was dispensed accurately into each flask, and the samples were subjected to extraction *via* ultrasonication (250 W, 53 kHz) for a duration of 30 min in an SK-8200HP ultrasonic water bath (Shanghai Kudos Ultrasonic Instrument Co., Ltd., Shanghai, China). Prior to injection, the ultimate extraction solution underwent filtration using a membrane filter with a pore size of 0.22 μm. The standard substances were precisely weighed and subsequently solubilized in 70 % methanol to create the stock solutions, all of which were maintained at 4 °C before use.

2.3.2. Preparation for ICP-MS analysis

Each powdered sample, weighing precisely 0.5 g, was meticulously added to pre-cleaned Teflon digestion vessels treated with nitric acid, after which 5 mL of concentrated nitric acid was added. Then, a Multiwave PRO microwave digestion system (Anton Paar, Graz, Austria) was used to digest the samples. The microwave temperature was increased gradually to 80 °C over 3 min, maintained for 10 min, increased to 130 °C over 3 min, maintained for 5 min, then increased to 180 °C over 15 min, and maintained for 8 min. Upon reaching ambient temperature, the digestion solution was diluted to volume in a volumetric flask with ultrapure water for elemental analysis. Blank solutions were formulated following the same procedure.

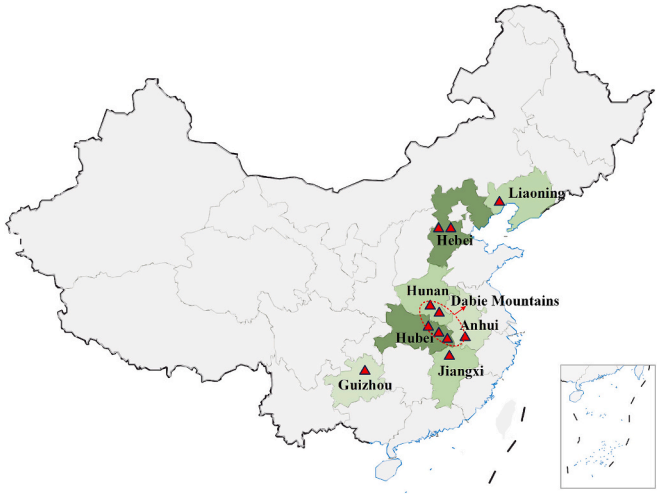

Fig. 1. Geographical information of AAF samples from seven provinces in China.

2.4. UHPLC analysis

Phenolic compounds (neochlorogenic acid, chlorogenic acid, cryptochlorogenic acid, caffeic acid, schaftoside, isoquercitrin, isochlorogenic acid B, cynarine, isochlorogenic acid A, isochlorogenic acid C, 3,4,5-tricaffeoylquinic acid, apigenin, hispidulin, jaceosidin, 5,7,3′-trihydroxy-6,4′,5′-trimethoxyflavone, eupatilin, and vitexicarpin) were isolated on a 1290 Infinity II LC System connected to a Variable Wavelength Detector (VWD). The column was an ACQUITY UPLC HSS T3 column (150 mm × 2.1 mm, 1.8 μm, Waters, MA, USA). Utilizing a flow rate of 0.3 mL/min, a mobile phase consisting of 0.1 % aqueous formic acid (A) (*v*/v) and acetonitrile (B) was employed. The elution protocol was executed according to a predefined linear gradient, as follows: 10 % B at 0 min; 20 % B at 7 min; 27 % B at 17 min; 33 % B at 22 min; 38 % B at 27 min; 60 % B at 29 min; 70 % B at 32 min; 90 % B at 33–35 min. Following a 5-min interval, the mobile phase was returned to its initial parameters. The column oven was maintained at a temperature of 30 °C, and a 1 μL injection volume was employed. Phenolic compounds were detected at a wavelength of 330 nm. The quantitative analysis was carried out using external standards, demonstrating correlation coefficients surpassing 0.9990 across all calibration curves. Identification and quantification of 17 phenolic compounds were achieved through retention time analysis and calculation of individual standard linear equations.

2.5. ICP-MS analysis

Mineral element content analysis, encompassing Na, Mg, Al, K, Ca, Cr, Mn, Fe, Co, Ni, Cu, Zn, As, Se, Cd, Ba, Hg, and Pb, was conducted utilizing ICAP RQ inductively coupled plasma mass spectrometry (Thermo Fisher Scientific, Bremen, Germany), following the guidelines stipulated in the Chinese Pharmacopeia (2020 Edition) (Commission, C. P., 2020). The instrument was typically operated under the following standard parameters: RF power: 1550 W, nebulizer pump: 40 rpm, sampling depth: 5.0 mm, carrier gas: 1.14 L/min, makeup gas: 0.80 L/min, CCT collision gas: 4.4 L/min, and cooling gas: 14.0 L/min, repeated two times. To correct for matrix effects and instrument drift, an internal standard containing Sc, Ge, Rh, In, Re, and Bi was employed. This internal standard (100 μg/L) was added to all samples and calibration standards. The R^2 value of the calibration curve was 0.9990 or higher for all elements; the LOD, LOQ, RSD, and recovery rate of each element are shown in Table S1. The reported results represent the average of two replicate measurements.

2.6. Statistical analysis

The phenolic chromatographic fingerprint was constructed using the Similarity Evaluation System for Chromatographic Fingerprint of TCM (Chinese Pharmacopeia Commission, Beijing, China). One-way analysis of variance (ANOVA), HCA, PCA, and Pearson's correlation analysis were performed using OriginPro 2024b (OriginLab Corporation, Northampton, MA, USA); the orthogonal partial least squares discriminant analysis (OPLS-DA) and receiver operating characteristic (ROC) analysis were executed using SIMCA 14.1 software (Umetrics, Umea, Sweden).

3. Results and discussion

3.1. Phenolic compounds of AAF samples from different geographical origins

Phenolic compounds, such as phenolic acids and flavonoids, are the main non-volatile components of AAF and possess various biological activities (Chang et al., 2022; Z. C. Wang et al., 2023). Seventeen phenolic compounds, including nine phenolic acids and eight flavonoids, were determined by UHPLC (Table 1 and Fig. 2A). The chromatogram in Fig. 2B illustrates the peaks corresponding to the 17 phenolic compounds present in both the samples and the reference

Table 1
The average concentrations of 17 phenolic compounds in AAF samples from various geographical origins.

Components	Geographical origins (mg/g, mean ± SD)						
	HUB (n = 30)	HN (n = 20)	AH (n = 10)	JX (n = 10)	GZ (n = 10)	HEB (n = 10)	LN (n = 10)
Neochlorogenic acid	$0.140^{f} \pm 0.055$	$0.370^{c} \pm 0.074$	$0.214^{e} \pm 0.011$	$0.544^{b} \pm 0.056$	$0.248^{de} \pm 0.019$	$0.287^{d} \pm 0.069$	$0.665^{a} \pm 0.023$
Chlorogenic acid	$0.855^{c} \pm 0.376$	$2.163^{b} \pm 0.669$	$1.067^{c} \pm 0.059$	$3.679^{a} \pm 0.285$	$2.306^{b} \pm 0.204$	$2.294^{b} \pm 0.156$	$4.182^{a} \pm 0.161$
Cryptochlorogenic acid	$0.161^{c} \pm 0.051$	$0.346^{b} \pm 0.085$	$0.298^{b} \pm 0.016$	$0.536^{a} \pm 0.039$	$0.214^{c} \pm 0.018$	$0.199^{c} \pm 0.015$	$0.356^{b} \pm 0.014$
Caffeic acid	$0.071^{c} \pm 0.066$	$0.091^{c} \pm 0.046$	$0.162^{b} \pm 0.011$	$0.234^{a} \pm 0.014$	$0.085^{c} \pm 0.01$	$0.121^{bc} \pm 0.043$	$0.112^{bc} \pm 0.013$
Schaftoside	$1.095^{ab} \pm 0.308$	$1.267^{a} \pm 0.459$	$0.541^{cd} \pm 0.060$	$0.607^{cd} \pm 0.392$	$0.336^{d} \pm 0.169$	$0.768^{bc} \pm 0.261$	$0.574^{cd} \pm 0.030$
Isoquercitrin	$0.425^{ab} \pm 0.168$	$0.363^{bc} \pm 0.174$	$0.407^{ab} \pm 0.042$	$0.112^{d} \pm 0.010$	$0.549^{a} \pm 0.052$	$0.225^{cd} \pm 0.010$	$0.173^{d} \pm 0.030$
Isochlorogenic acid B	$2.870^{bc} \pm 1.191$	$4.768^{a} \pm 1.512$	$3.091^{bc} \pm 0.141$	$5.297^{a} \pm 0.56$	$3.135^{bc} \pm 0.301$	$2.099^{c} \pm 0.198$	$3.615^{b} \pm 0.238$
Cynarine	$0.177^{e} \pm 0.071$	$0.420^{d} \pm 0.150$	$0.158^{e} \pm 0.012$	$0.345^{d} \pm 0.021$	$0.574^{c} \pm 0.076$	$1.467^{b} \pm 0.296$	$1.761^{a} \pm 0.082$
Isochlorogenic acid A	$5.737^{c} \pm 3.416$	$7.713^{b} \pm 1.711$	$6.280^{bc} \pm 0.157$	$11.378^{a} \pm 0.867$	$11.360^{a} \pm 1.198$	$7.297^{bc} \pm 0.906$	$11.883^{a} \pm 0.482$
Isochlorogenic acid C	$2.484^{d} \pm 1.083$	$3.657^{b} \pm 0.691$	$5.264^{a} \pm 0.170$	$5.214^{a} \pm 0.311$	$2.834^{cd} \pm 0.231$	$2.352^{d} \pm 0.184$	$3.397^{bc} \pm 0.147$
3,4,5-Tricaffeoylquinic acid	$1.855^{a} \pm 1.272$	$1.783^{ab} \pm 1.057$	$0.813^{bc} \pm 0.060$	$0.405^{c} \pm 0.110$	$1.098^{abc} \pm 0.101$	$1.562^{abc} \pm 0.342$	$1.472^{abc} \pm 0.089$
Apigenin	$0.014^{ab} \pm 0.005$	$0.006^{c} \pm 0.004$	$0.018^{a} \pm 0.016$	$0.009^{bc} \pm 0.005$	$0.007^{bc} \pm 0.003$	$0.004^{c} \pm 0.001$	$0.004^{c} \pm 0.000$
Hispidulin	$0.056^{b} \pm 0.015$	$0.046^{c} \pm 0.007$	$0.108^{a} \pm 0.006$	$0.039^{cd} \pm 0.004$	$0.031^{d} \pm 0.012$	ND	$0.031^{d} \pm 0.002$
Jaceosidin	$0.304^{b} \pm 0.078$	$0.306^{b} \pm 0.037$	$0.443^{a} \pm 0.016$	$0.279^{bc} \pm 0.014$	$0.128^{d} \pm 0.017$	$0.048^{e} \pm 0.010$	$0.248^{c} \pm 0.030$
5,7,3′-Trihydroxy-6,4′,5′-trimethoxyflavone	$0.118^{b} \pm 0.049$	$0.090^{c} \pm 0.023$	$0.301^{a} \pm 0.011$	$0.053^{d} \pm 0.022$	$0.053^{d} \pm 0.007$	$0.011^{e} \pm 0.015$	$0.027^{de} \pm 0.012$
Eupatilin	$1.568^{b} \pm 0.201$	$1.232^{c} \pm 0.171$	$2.640^{a} \pm 0.145$	$1.145^{c} \pm 0.044$	$0.572^{d} \pm 0.078$	$0.214^{e} \pm 0.038$	$0.705^{d} \pm 0.054$
Vitexicarpin	$0.637^{b} \pm 0.158$	$0.468^{c} \pm 0.069$	$0.781^{a} \pm 0.034$	$0.672^{ab} \pm 0.036$	$0.180^{e} \pm 0.0170$	$0.140^{e} \pm 0.016$	$0.352^{d} \pm 0.034$

Samples originated from: Hubei Province (HUB), Henan Province (HN), Anhui Province (AH), Jiangxi Province (JX), Guizhou Province (GZ), Hebei Province (HEB), and Liaoning Province (LN). Note: Letters "a"–"f" within identical lines denote statistically significant differences ($P < 0.05$). ND denotes undetectable content. There was a notable difference in the contents of phenolic compounds among all of the geographically distinct samples ($P < 0.001$).

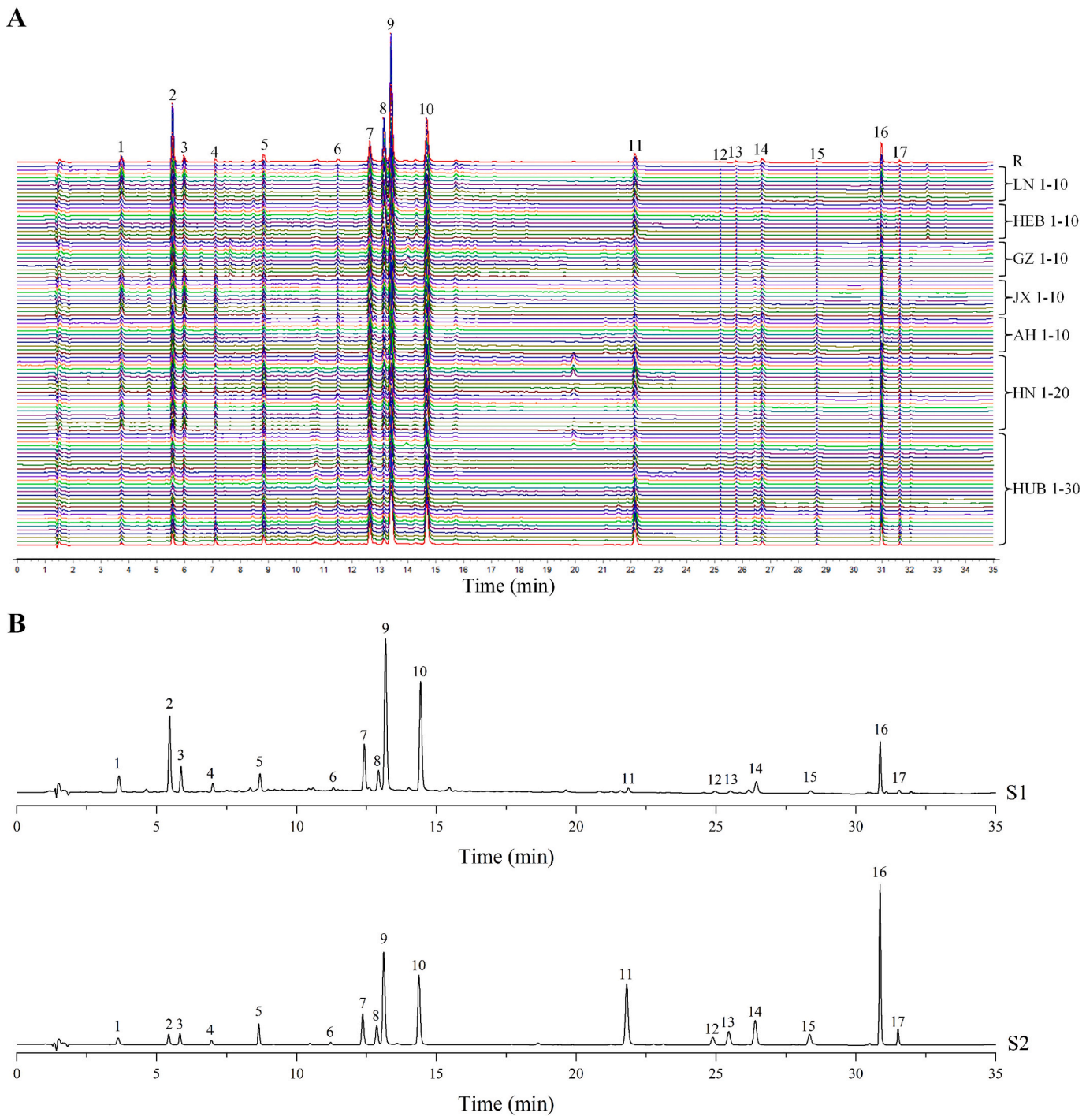

Fig. 2. UHPLC analysis of 100 batches of AAF samples from seven provinces in China. (A) UHPLC fingerprints of 100 batches of AAF samples and the reference fingerprint (R); (B) UHPLC chromatograms of AAF sample (S1) and reference solution (S2). Peaks 1 to 17 represent neochlorogenic acid, chlorogenic acid, cryptochlorogenic acid, caffeic acid, schaftoside, isoquercitrin, isochlorogenic acid B, cynarine, isochlorogenic acid A, isochlorogenic acid C, 3,4,5-tricaffeoylquinic acid, apigenin, hispidulin, jaceosidin, 5,7,3′-trihydroxy-6,4′,5′-trimethoxyflavone, eupatilin, and vitexicarpin.

solution. Peaks 1–17 were characterized as neochlorogenic acid, chlorogenic acid, cryptochlorogenic acid, caffeic acid, schaftoside, isoquercitrin, isochlorogenic acid B, cynarine, isochlorogenic acid A, isochlorogenic acid c, 3,4,5-tricaffeoylquinic acid, apigenin, hispidulin, jaceosidin, 5,7,3′-trihydroxy-6,4′,5′-trimethoxyflavone, eupatilin, and vitexicarpin, respectively. The mean concentrations of these 17 compounds were compared among AAF samples from different origins using analysis of variance (ANOVA), and the results from the analysis of these concentration differences are depicted using box plots (Fig. S1). The findings revealed a notable distinction (with a confidence level of 95 %) in the contents of phenolic compounds among all of the geographically distinct samples ($P < 0.001$), indicating that the origin impacts the levels of these constituents. Samples from AH exhibited the highest mean concentrations of isochlorogenic acid C, apigenin, hispidulin, jaceosidin, 5,7,3′-trihydroxy-6,4′,5′-trimethoxyflavone, eupatilin, and vitexicarpin at 5.264 mg/g, 0.018 mg/g, 0.108 mg/g, 0.443 mg/g, 0.301 mg/g, 2.640 mg/g and 0.781 mg/g, respectively. The JX samples demonstrated higher mean values for most phenolic acids, while the concentrations of

flavonoids in HEB and LN were comparatively lower.

3.2. Chemometric analysis of phenolic compounds in AAF samples from diverse geographical origins

3.2.1. HCA of phenolic compounds

The HCA of 17 phenolic compounds in 100 batches of AAF samples from different origins was carried out using a heat map (Fig. 3A), and the samples were found to be clustered into seven regions. The samples from the neighboring provinces of HUB and HN were similar, while the remaining samples could be distinguished by province. JX was quite different from samples originating in three other provinces in central China (HUB, HN, and AH), but GZ, JX, and those from northern China (HEB and LN) were similar.

The 17 phenolic compounds were clustered into four groups. The contents of group 1 (neochlorogenic acid, chlorogenic acid, isochlorogenic acid A, and cynarine) were higher in JX and LN; the contents of group 2 (cryptochlorogenic acid, caffeic acid, isochlorogenic acid B, and isochlorogenic acid C) were higher in JX; the contents of group 3 (schaftoside, 3,4,5-tricaffeoylquinic acid, and isoquercitrin) were higher in HUB and HN but lower in JX, LN, and AH; and the contents of group 4 (apigenin, hispidulin, eupatilin, 5,7,3′-trihydroxy-6,4′,5′-trimethoxyflavone, jaceosidin, and vitexicarpin) were higher in AH. Most compounds in groups 1 and 2 were phenolic acids, while groups 3 and 4 were composed mainly of flavonoids. The clustering results were related to differences in the contents of each group of compounds.

3.2.2. PCA of phenolic compounds

A PCA was used to analyze the phenolic compound contents across samples from different origins. The cumulative variance contribution of the first three principal components (PCs) was 76.46 %. The initial principal component (PC1) elucidated 37.34 % of the overall variance, while the subsequent two PCs (PC2 and PC3) contributed 25.79 % and 13.33 %, respectively. As illustrated in Fig. 3B, the scores derived from PC1, PC2, and PC3, revealed seven distinct groups. The samples could, therefore, be distinguished effectively according to their province of origin. The confidence ellipses of HUB and HN samples partially overlapped, and the loadings of the phenolic compounds were divided into four groups. The comparison of the phenolic contents in samples from different provinces is displayed in a biplot—the results from the PCA were similar to those from the HCA, with geographically adjacent samples being relatively closer.

3.2.3. OPLS-DA and ROC of phenolic compounds

OPLS-DA is recognized as a highly effective approach for sample classification and the establishment of discriminant models, thus warranting its selection as a pivotal indicator in endeavors aimed at discriminating geographical origins (Du et al., 2021; Hye Hur et al., 2023). In the current study, the OPLS-DA was conducted on 17 phenolic compounds within a dataset comprising 80 AAF samples (80 % of the AAF samples from each geographical origin were chosen randomly). As illustrated in Fig. 3C, no overlap was observed among the seven groups of samples originating from distinct sources, indicating that the discrimination was excellent. The model exhibited favorable parameter values, with R^2X, R^2Y, and Q^2Y values of 0.968, 0.843, and 0.800, respectively, indicating a robust fit and satisfactory predictive capability (Kang et al., 2022). After conducting 200 iterations of permutation tests (Fig. S2), the intercepts of R^2 and Q^2 were found to be below 0.3 and 0.05, respectively, signifying the absence of overfitting in the model (Long et al., 2023; Yu et al., 2023). The associations between the phenolic compounds and AAF samples are depicted in Fig. 3D. An inverse relationship between phenolic compound concentrations in the samples and the distances between their origins was observed (Mi et al., 2022). For example, the flavonoids including jaceosidin, 5,7,3′-trihydroxy-6,4′,5′-trimethoxyflavone, hispidulin, apigenin, eupatilin, and vitexicarpin were distributed closely around the AAF samples from AH; the phenolic acids including cryptochlorogenic acid, caffeic acid, isochlorogenic acid B, and Isochlorogenic acid A were distributed closely around the AAF samples from JX; schaftoside, 3,4,5-tricaffeoylquinic acid, apigenin, and isoquercitrin were distributed closely around the AAF samples from HUB; and the maximum concentrations of these components were identified in each respective geographical origin.

Generally, variables with a variable importance in projection (VIP) > 1 are regarded as pivotal in discriminating between diverse sample groups (Lu et al., 2024; X. C. Song et al., 2021). Six phenolic components with VIP > 1 were subjected to screening by OPLS-DA (Fig. 3E): cynarine, vitexicarpin, schaftoside, caffeineic acid, isochlorogenic acid B, and 5,7,3′-trihydroxy-6,4′,5′-trimethoxyflavone.

The accuracy of the OPLS-DA model at discriminating AAF samples from different geographical origins was evaluated using the ROC curve of the phenolic compounds (Mi et al., 2019; Mi et al., 2022). The areas under the ROC curve (AUC) for HUB and HN were 0.995 and 0.997, respectively, while the AUC for all other origins was 1 (Fig. 3F), indicating the robust discriminatory capacity of the phenolic compound contents in separating AAF samples from seven provinces (Yoon et al., 2022).

3.3. Mineral elements in AAF samples from different geographical origins

ICP-MS offers the benefits of heightened sensitivity, concurrent analysis of numerous elements, and expedited analysis. Such multi-element analyses hold promise for distinguishing geographical origins effectively (Mi et al., 2022; Yu et al., 2023; H. R. Zhang, Liu, et al., 2021). Eighteen chemical elements were quantitatively determined in AAF samples from different geographical origins. The most highly concentrated element in 100 batches of AAF samples was K, followed by Ca, Mg, Fe, Al, and Mn, while the contents of other elements remained relatively low (Table 2). ANOVA was utilized to assess the differences in the mean values of the 18 mineral elements among AAF samples from various origins. Comparations of the contents of mineral elements between samples of different geographical origins (seven provinces) are indicated in box plots (Fig. S3). The mean values of K, Mn, Ni, Zn, Cd, and Ba were highest in JX samples, whereas the mean values of Mg, Al, Cr, Co, Zn, and As in HUB were lower. The levels of the 18 mineral elements exhibited significant variation (at the 95 % confidence level, $P < 0.001$) across the different geographical origins, indicating that the environmental differences between the places of origin affected the contents of mineral elements in AAF.

3.4. Chemometric analysis of mineral elements in AAF samples from different origins

3.4.1. HCA of mineral elements

The HCA of 18 mineral elements in 100 batches of AAF samples from different origins was carried out using a heat map (Fig. 4A), and the samples were clustered into seven groups. The samples from the Dabie Mountain region (HUB, HN, and AH) exhibited a relatively high degree of similarity, while the other samples could be distinguished according to the provinces from which they originated. Similar to the clustering of the phenolic compounds, the samples from JX were distinct from those of the three provinces surrounding the Dabie Mountains (HUB, HN, and AH).

The 18 mineral elements were grouped into five clusters. Group 1 elements (Na, Al, Fe, Co, Cr, and Pb) were found at higher concentrations in the HEB and LN samples, while HUB and JX contained lower levels. The group 2 (Mg and As) contents were found to be higher in GZ, LN, and HEB samples, and the contents of group 3 (Hg and Ca) were also found to be higher in HEB samples. Group 4 elements (K, Mn, Cd, Ni, Zn, and Se) were found at higher levels in JX but lower levels in GZ samples. Finally, the concentrations of group 5 elements (Cu and Ba) were higher in the HUB and JX samples.

The range of mineral elements found in samples from adjacent

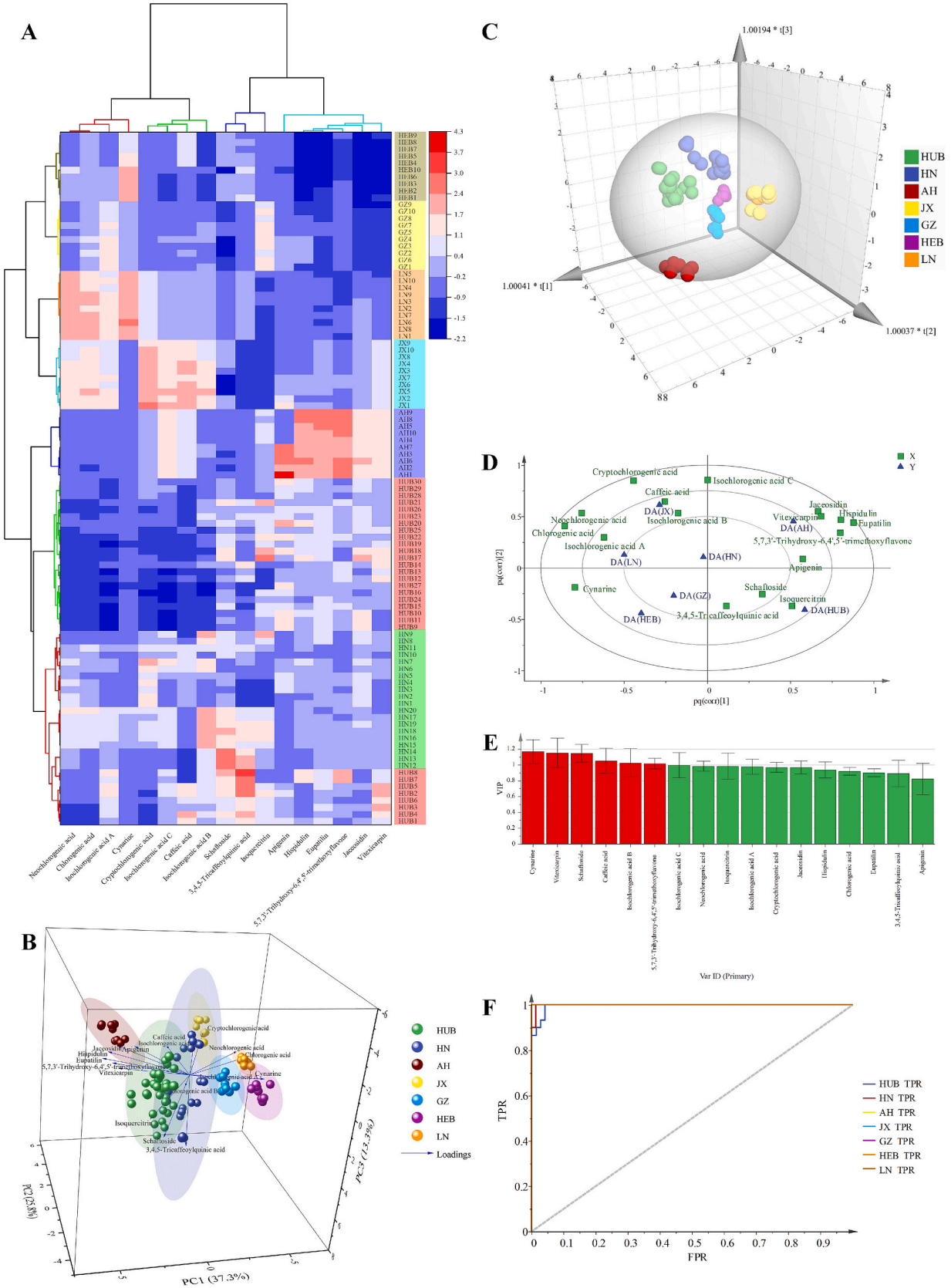

Fig. 3. Chemometric analysis of phenolic compounds in AAF samples from different geographical origins. (A) Pearson's correlation plot of the contents of 17 phenolic compounds. (A) Heat map analysis of the HCA classification of AAF samples and 17 phenolic compounds. (B) Biplot of the PCA of AAF samples from seven provinces and 17 phenolic compounds. (C) OPLS-DA score scatter plot. (D) Correlation circle between phenolic compounds and AAF samples. (E) VIP scores plot. (F) ROC curve of OPLS-DA (phenolic compounds).

Table 2
The average concentrations of the 18 mineral elements in AAF samples originating from various geographical origins.

Elements	Geographical origins (mg/g, mean ± SD)						
	HUB (n = 30)	HN (n = 20)	AH (*n* = 10)	JX (n = 10)	GZ (n = 10)	HEB (n = 10)	LN (n = 10)
Na	$17.61^{b} \pm 13.36$	$52.44^{a} \pm 27.96$	$25.97^{b} \pm 7.79$	$11.3^{b} \pm 3.4$	$9.28^{b} \pm 5.59$	$48.68^{a} \pm 3.81$	$52.78^{a} \pm 8.39$
Mg	$2265.68^{d} \pm 367.74$	$2682.69^{c} \pm 227.48$	$3065.05^{b} \pm 169.16$	$1730.61^{e} \pm 74.11$	$3983.36^{a} \pm 198.19$	$2973.59^{bc} \pm 110.90$	$2828.44^{bc} \pm 139.78$
Al	$238.45^{d} \pm 67.55$	$425.41^{b} \pm 94.22$	$275.75^{cd} \pm 34.21$	$199.97^{d} \pm 23.32$	$356.07^{bc} \pm 27.10$	$782.19^{a} \pm 87.42$	$824.92^{a} \pm 48.62$
K	$30,682.70^{ab} \pm 4395.60$	$32,565.18^{a} \pm 4827.15$	$28,220.13^{b} \pm 1097.01$	$34,348.95^{a} \pm 2046.29$	$30,219.21^{ab} \pm 721.05$	$23,097.90^{c} \pm 1225.16$	$31,429.48^{ab} \pm 1233.38$
Ca	$10,657.84^{b} \pm 1282.71$	$10,049.97^{bc} \pm 789.17$	$9607.29^{c} \pm 374.02$	$6819.18^{d} \pm 401.09$	$10,605.88^{bc} \pm 150.62$	$12,029.27^{a} \pm 456.97$	$9978.58^{bc} \pm 227.28$
Cr	$3.34^{de} \pm 1.78$	$5.28^{c} \pm 1.40$	$4.58^{cd} \pm 0.89$	$2.86^{de} \pm 0.83$	$2.10^{e} \pm 0.13$	$11.39^{a} \pm 0.82$	$8.58^{b} \pm 0.73$
Mn	$186.37^{b} \pm 86.88$	$175.21^{b} \pm 60.73$	$125.53^{bc} \pm 6.80$	$594.83^{a} \pm 57.03$	$160.20^{bc} \pm 3.76$	$92.67^{c} \pm 6.51$	$155.93^{bc} \pm 16.06$
Fe	$314.06^{cd} \pm 93.91$	$515.15^{b} \pm 178.00$	$401.16^{bc} \pm 42.94$	$236.85^{d} \pm 22.28$	$366.56^{cd} \pm 19.21$	$995.55^{a} \pm 111.76$	$1114.56^{a} \pm 128.46$
Co	$0.20^{e} \pm 0.070$	$0.26^{d} \pm 0.04$	$0.30^{cd} \pm 0.03$	$0.26^{d} \pm 0.07$	$0.34^{c} \pm 0.02$	$0.45^{b} \pm 0.04$	$0.52^{a} \pm 0.04$
Ni	$2.66^{c} \pm 1.22$	$3.47^{b} \pm 0.57$	$2.76^{bcd} \pm 0.15$	$4.83^{a} \pm 0.22$	$0.97^{e} \pm 0.02$	$1.47^{e} \pm 0.13$	$1.84^{de} \pm 0.09$
Cu	$18.88^{a} \pm 4.91$	$15.28^{bc} \pm 1.06$	$13.21^{bcd} \pm 0.72$	$17.01^{ab} \pm 1.75$	$11.59^{d} \pm 0.32$	$13.17^{cd} \pm 0.39$	$13.02^{cd} \pm 0.44$
Zn	$38.82^{c} \pm 8.95$	$46.58^{ab} \pm 5.00$	$33.54^{cd} \pm 3.15$	$51.93^{a} \pm 3.76$	$31.87^{d} \pm 2.98$	$36.19^{cd} \pm 4.62$	$39.67^{bcd} \pm 4.65$
As	$0.22^{d} \pm 0.07$	$0.29^{c} \pm 0.05$	$0.20^{d} \pm 0.01$	$0.31^{c} \pm 0.06$	$0.65^{a} \pm 0.06$	$0.49^{b} \pm 0.06$	$0.65^{a} \pm 0.04$
Se	$0.91^{c} \pm 0.31$	$1.17^{b} \pm 0.31$	$0.67^{cd} \pm 0.05$	$1.43^{ab} \pm 0.16$	$0.58^{d} \pm 0.03$	$1.46^{a} \pm 0.21$	$1.43^{ab} \pm 0.1$
Cd	$0.58^{c} \pm 0.36$	$0.81^{b} \pm 0.24$	$0.28^{d} \pm 0.01$	$1.36^{a} \pm 0.07$	$0.49^{cd} \pm 0.03$	$0.22^{d} \pm 0.02$	$0.27^{d} \pm 0.02$
Ba	$47.55^{ab} \pm 11.42$	$41.55^{b} \pm 5.77$	$41.60^{ab} \pm 1.59$	$50.40^{a} \pm 8.67$	$9.06^{d} \pm 0.41$	$26.41^{c} \pm 2.17$	$27.24^{c} \pm 1.72$
Hg	$0.016^{b} \pm 0.004$	$0.022^{a} \pm 0.011$	$0.018^{ab} \pm 0.003$	$0.014^{b} \pm 0.003$	$0.018^{ab} \pm 0.002$	$0.020^{ab} \pm 0.003$	$0.013^{b} \pm 0.003$
Pb	$1.08^{cd} \pm 0.35$	$1.31^{bc} \pm 0.31$	$1.01^{cd} \pm 0.07$	$0.83^{d} \pm 0.07$	$1.10^{cd} \pm 0.06$	$1.45^{b} \pm 0.15$	$2.12^{a} \pm 0.23$

Note: Letters "a"–"f" within lines denote statistically significant differences ($P < 0.05$). The levels of the 18 mineral elements exhibited significant variation (at the 95 % confidence level, $P < 0.001$) across the different geographical origins.

geographical origins was similar. However, the influence of rivers on element distribution was significant. For instance, although relatively close in distance, the sample collection site in JX Province was situated south of the Yangtze River, distinct from the other three provinces north of the Yangtze River (Dabie Mountains).

3.4.2. PCA of mineral elements

The cumulative variance contribution of the first four PCs was 79.35 %. The initial principal component (PC1) elucidated 39.91 % of the overall variance, while the subsequent three PCs (PC2, PC3, and PC4) contributed 21.69 %, 10.70 %, and 7.05 %, respectively. As illustrated in Fig. 4B, the comparison of mineral elements in samples from different provinces is directly displayed in biplots; the PC1, PC2, and PC3 scores indicated the presence of seven distinct groups. The samples from JX, GX, HEB, and AH were distinguished effectively according to their provinces of origin, while the scores and confidence ellipses of samples from the Dabie Mountain region (HUB, HN, and AH) partially overlapped. The loadings of the mineral elements were divided into five groups; the biplot visually presents the distribution of mineral elements, indicating that the geographical origin of the samples significantly influences their concentrations, as revealed by the PCA analysis.

3.4.3. OPLS-DA and ROC of mineral elements

The OPLS-DA was applied to 18 mineral elements within a dataset of 80 AAF samples (80 % of the AAF samples from each geographical origin were randomly chosen from the whole sample). The results from the samples originating in the Dabie Mountain region (HUB, HN, and AH) partially overlapped when analyzed according to the seven provinces (Fig. 4C). However, the OPLS-DA discriminated well between samples from five regions, the Dabie Mountain region, JX, GZ, HEB, and LN, indicating its effectiveness (Fig. 4D). Moreover, the values of the model parameters R^2X, R^2Y, and Q^2Y were 0.928, 0.847, and 0.803, respectively, demonstrating that the model had strong explanatory and predictive capacity (Kang et al., 2022). After conducting 200 iterations of the permutation tests (Fig. S4), the intercepts of R^2 and Q^2 were found to be below 0.3 and 0.05, respectively, signifying the absence of overfitting in the model (Yu et al., 2023). The correlations between mineral elements and AAF samples are illustrated in Fig. 4E. For instance, elements including K, Mn, Cu, Zn, Ni, Ba, and Cd were distributed closely around the AAF samples from JX, with the maximum concentration levels observed in samples originating from this region. Ten mineral elements with VIP > 1 were screened out by OPLS-DA (Fig. 4F): Mn, As, Pb, Cr, Ba, Mg, Se, Ca, K, and Fe.

The accuracy of the OPLS-DA model at discriminating AAF samples from different geographical origins was evaluated using the mineral element ROC curve (Mi et al., 2019; Mi et al., 2022). The perfect classification performance, as evidenced by an AUC of 1 (Fig. 4G), underscored the robust discriminatory capacity of the mineral element content to distinguish between AAF samples from five regions.

3.5. Prediction of geographical origin

OPLS-DA, utilizing phenolic compound and mineral element concentrations, successfully distinguished AAF samples from diverse geographical origins. To assess the robustness of the supervised models regarding phenolic compounds and mineral elements, a subset comprising 20 % of the samples was reserved for testing purposes to validate the accuracy of the models. Integration of the remaining 20 AAF samples with documented data (test set) and the 80 AAF samples from the discriminant models yielded a dataset of 100 samples (20 + 80) used to develop the OPLS-DA models. The developed model was subsequently tested using the test set to evaluate its robustness and predictive performance in classification. As illustrated in Table 3, all samples were accurately predicted, and the accuracy of the two constructed models was 100 %, exhibiting excellent predictability. Combining the quantitative analysis of phenolic compounds and mineral elements with chemometrics to classify the geographical origins of AAF may be a reliable method and has great application potential.

3.6. Correlation analysis between phenolic compounds and mineral elements of AAF

Pearson's correlation analysis was utilized to elucidate the intricate interrelations among the concentrations of the 17 phenolic compounds and 18 mineral elements. The correlation coefficients indicated that, of 595 pairs analyzed, 383 pairs met the threshold of $P < 0.05$ (Fig. 5). Within this subset, 308 pairs exhibited statistically significant positive correlations ($R > 0$), while 287 pairs displayed significant negative correlations ($R < 0$).

A significant positive relationship was observed between the concentrations of neochlorogenic acid, chlorogenic acid, cryptochlorogenic acid, caffeic acid, isochlorogenic acid B, isochlorogenic acid A and

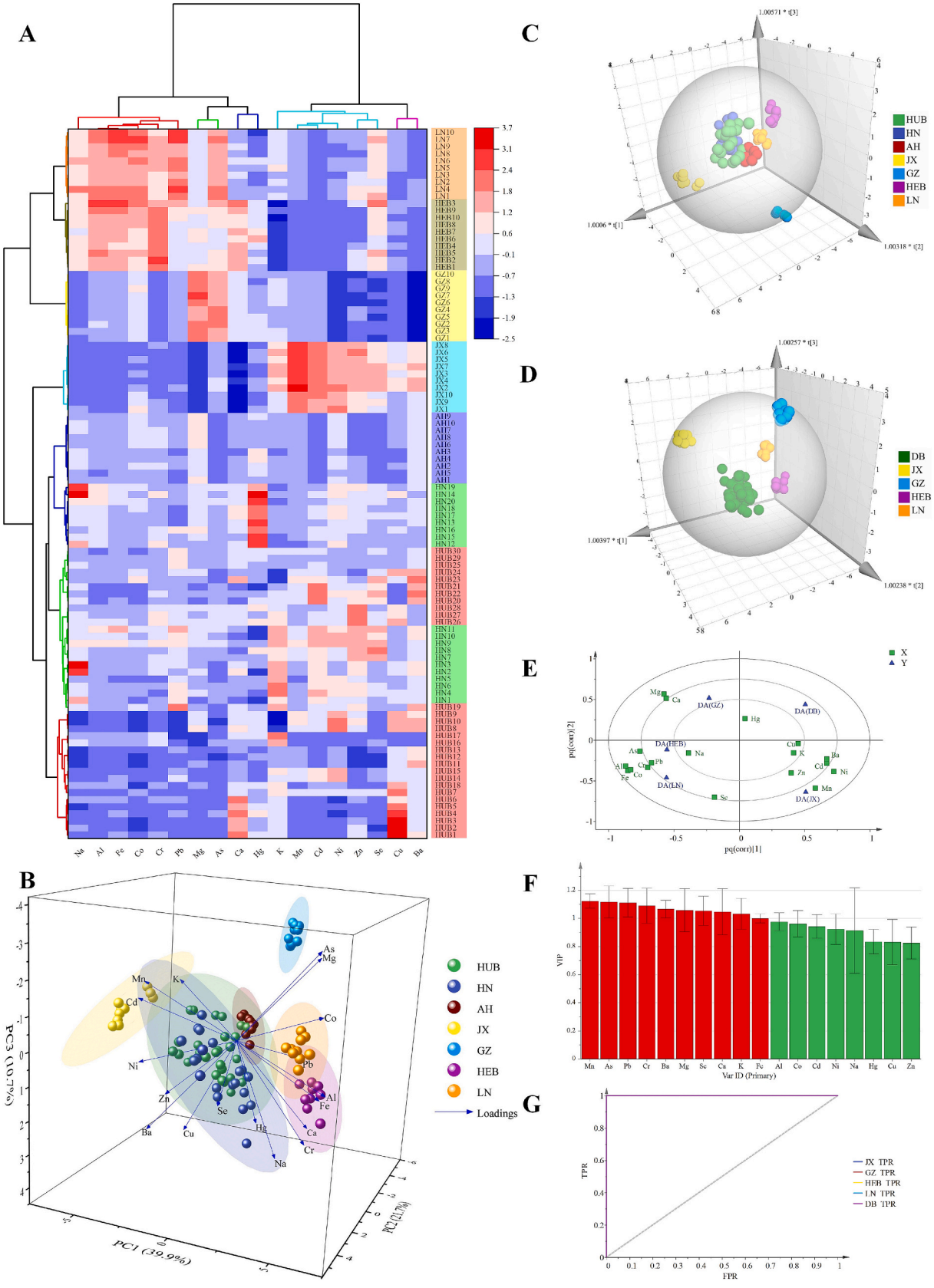

Fig. 4. Chemometric analysis of mineral elements in AAF samples from different geographical origins. (A) Heat map analysis of HCA classification of AAF samples and 18 mineral elements. (B) Biplot of PCA of AAF samples from 7 provinces and 18 mineral elements. (C) OPLS-DA score scatter plot (seven provinces). (D) OPLS-DA score scatter plot (five regions). Dabie Mountain region (DB). (E) Correlation circle between mineral elements and AAF samples. (F) VIP scores plot. (G) ROC curve of OPLS-DA (mineral elements).

Table 3
The prognostication of documented data regarding AAF samples through the developed OPLS-DA models of phenolic components (a) and mineral elements (b).

(a)									
Test Set	Members	Accuracy (%)	HUB	HN	AH	JX	GZ	HEB	LN
HUB	6	100 %	6	0	0	0	0	0	0
HN	4	100 %	0	4	0	0	0	0	0
AH	2	100 %	0	0	2	0	0	0	0
JX	2	100 %	0	0	0	2	0	0	0
GZ	2	100 %	0	0	0	0	2	0	0
HEB	2	100 %	0	0	0	0	0	2	0
LN	2	100 %	0	0	0	0	0	0	2
Total	20	100 %	6	4	2	2	2	2	2
(b)									
Test Set	Members	Accuracy (%)	DB			JX	GZ	HEB	LN
DB	12	100 %	12			0	0	0	0
JX	2	100 %	0			2	0	0	0
GZ	2	100 %	0			0	2	0	0
HEB	2	100 %	0			0	0	2	0
LN	2	100 %	0			0	0	0	2
Total	20	100 %	12			2	2	2	2

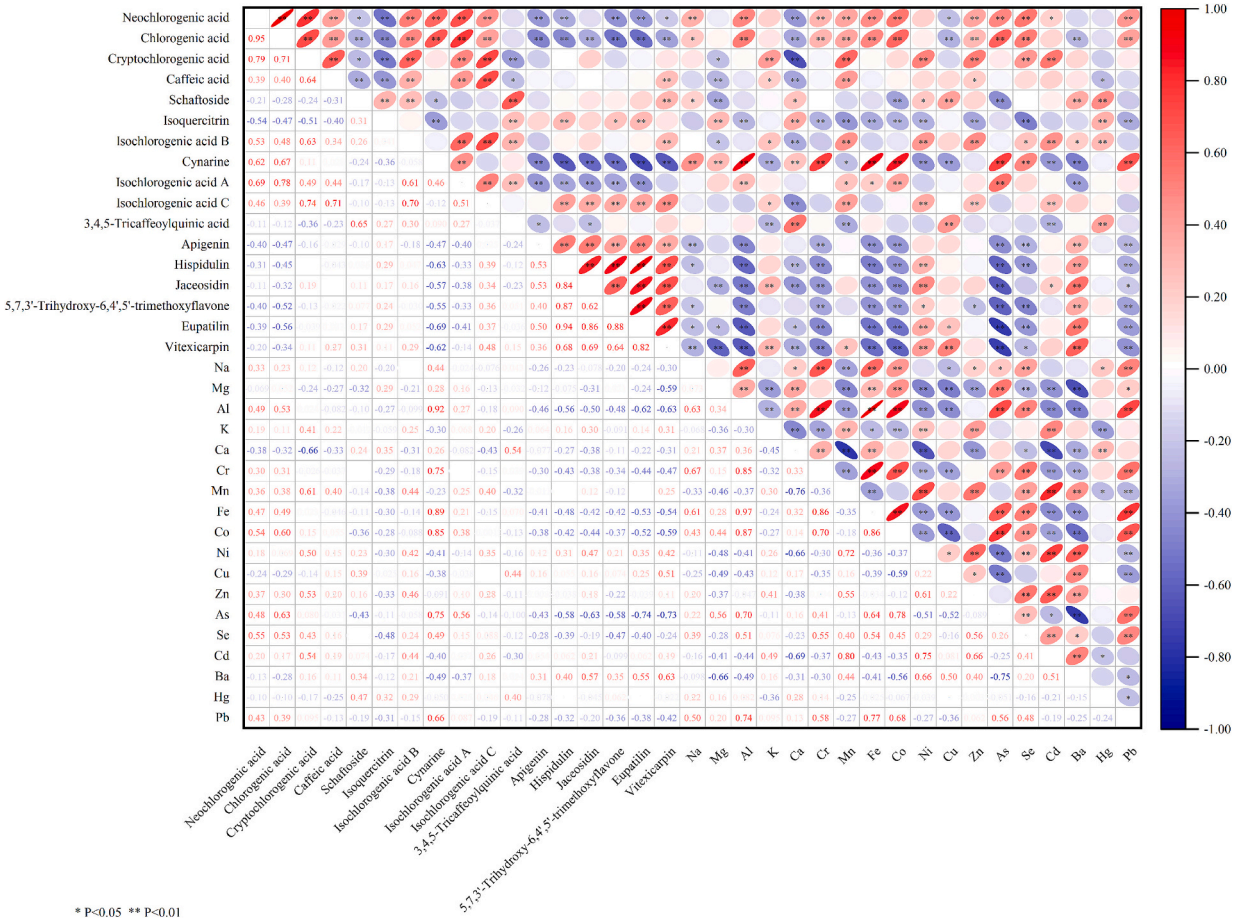

Fig. 5. Correlation coefficients between the contents of phenolic compounds and mineral elements in AAF.

isochlorogenic acid C. Likewise, the contents of apigenin, hispidulin, jaceosidin, 5,7,3′-trihydroxy-6,4′,5′-trimethoxyflavone, eupatilin, and vitexicarpin were significantly positively correlated. The 3,4,5-tricaffeoylquinic acid content was significantly positively correlated with schaftoside and isoquercitrin. The concentrations of neochlorogenic acid, chlorogenic acid, cynarine, and isochlorogenic acid A exhibited a negative correlation with the flavonoid content.

A positive relationship was observed between Na, Mg, Al, Ca, Cr, Fe, Co, and Pb contents. Likewise, the contents of K, Mn, Ni, Cu, Zn, Se, Cd, and Ba exhibited a positive correlation. The Se content was significantly positively correlated with Na, Al, Cr, Mn, Fe, Co, Ni, Zn, As, Cd, Ba, and Pb.

Furthermore, a significant correlation was observed between the contents of phenolic compounds and certain mineral elements in AAF. Each phenolic compound was found to be associated with 6 to 16 elements. For instance, the contents of five flavonoids (hispidulin, jaceosidin, 5,7,3′-trihydroxy-6,4′,5′-trimethoxyflavone, eupatilin, and vitexicarpin) exhibited a significantly positive correlation with Ni and Ba, while displaying a significantly negative correlation with Al, Cr, Fe, Co, As, and Pb. The contents of neochlorogenic acid and chlorogenic

acid exhibited a significant positive correlation with Na, Al, Cr, Mn, Fe, Co, Zn, As, Se, and Pb, while exhibiting a significant negative correlation with Ca and Cu. Additionally, Se was negatively correlated with all flavonoids in AAF except for schaftoside. K demonstrated a significant positive correlation with jaceosidin and eupatilin, caffeic acid, cryptochlorogenic acid, isochlorogenic acid B, and isochlorogenic acid C.

The content of inorganic elements in plants has been shown to affect the accumulation of active components, thus influencing plant quality (Wei et al., 2024; Ye et al., 2023). Here, complex correlations were observed between the contents of various phenolic compounds and mineral elements, which may be attributed to environmental influences, such as differences in soil composition across distinct origins.

4. Conclusions

In this study, chemometric analyses and the quantification of phenolic compounds and mineral elements were used to distinguish AAF samples from different geographical origins. The results showed that the contents of phenolic compounds and mineral elements varied greatly among the samples. The two methods offer great potential for identifying and predicting the geographical origin of AAF samples and are suitable for tracing their source. OPLS-DA emphasized that the classification and discrimination performance of a supervised modeling method was better than that of unsupervised modeling methods, especially for samples from similar geographical origins. The phenolic constituents and mineral elements differed in their suitability for use in classifying and distinguishing samples. The phenolic constituents were more useful for classifying samples from adjacent origins. Analysis of the phenolic compounds enabled samples from seven provinces to be distinguished effectively, while analysis of the mineral element levels was useful for distinguishing between samples from the areas surrounding the Dabie Mountains (HUB, HN, and AH) and the other four provinces. Using the ROC curve, the classification accuracies for the two OPLS-DA models were 0.995 or higher. Furthermore, the developed OPLS-DA models were validated using an independent test set of 20 samples with 100 % accuracy. Complex correlations were observed between the contents of various phenolic compounds and mineral elements in AAF, with the mineral elements possibly affecting the accumulation of phenolic compounds. This study demonstrates the efficacy of chemometric analysis, in conjunction with quantitative determination of phenolic compounds and mineral elements, as a viable strategy for identifying the geographic origin of AAF samples and provides a basis for assessing the differences in the characteristics of AAF samples originating from different regions. It also provides some insights into mineral element application strategies in the cultivation of *A. argyi*. However, there are still some limitations to the current research. The mechanisms by which mineral elements influence the accumulation of phenolic components in AAF require further investigation. Additionally, there is a need to develop more effective methods of evaluating AAF quality and tracing its origin. Our research group is actively exploring the use of near-infrared spectroscopy (NIRS) for rapid qualitative and quantitative analysis of AAF.

CRediT authorship contribution statement

Lifei Hu: Writing – original draft, Software, Investigation, Conceptualization. **Fengxiao Zhu:** Writing – review & editing, Validation, Data curation. **Yifan Wang:** Writing – review & editing, Validation, Data curation. **Tao Wu:** Writing – review & editing, Methodology. **Xin Wu:** Writing – review & editing, Methodology. **Zhian Huang:** Writing – review & editing, Data curation. **Daihua Sun:** Supervision, Resources, Conceptualization. **Mingxing Liu:** Writing – review & editing, Validation, Supervision, Conceptualization.

Declaration of competing interest

The authors declare that they have no known competing financial interests or personal relationships that could have appeared to influence the work reported in this paper.

Data availability

Data will be made available on request.

Acknowledgements

This work was supported by the Hubei Science and Technology Major Project, China(No. 2020ACA007, 2022ACA003)

Supplementary data

Supplementary data to this article can be found online at https://doi.org/10.1016/j.fochx.2024.101909.

References

Campmajó, G., Rodríguez-Javier, L. R., Saurina, J., & Núñez, O. (2021). Assessment of paprika geographical origin fraud by high-performance liquid chromatography with fluorescence detection (HPLC-FLD) fingerprinting. *Food Chemistry, 352*, Article 129397. https://doi.org/10.1016/j.foodchem.2021.129397

Chang, Y. Q., Fan, W. X., Shi, H., Feng, X., Zhang, D., Wang, L., … Guo, L. (2022). Characterization of phenolics and discovery of α-glucosidase inhibitors in *Artemisia argyi* leaves based on ultra-performance liquid chromatography-tandem mass spectrometry and relevance analysis. *Journal of Pharmaceutical and Biomedical Analysis, 220*, Article 114982. https://doi.org/10.1016/j.jpba.2022.114982

Chang, Y. Q., Zhang, D., Yang, G. Y., Zheng, Y. G., & Guo, L. (2021). Screening of anti-lipase components of *Artemisia argyi* leaves based on Spectrum-effect relationships and HPLC-MS/MS. *Frontiers in Pharmacology, 12*, Article 675396. https://doi.org/10.3389/fphar.2021.675396

Chen, J. K., Kuo, C. H., Kuo, W. W., Day, C. H., Wang, T. F., Ho, T. J., … Lu, C. Y. (2022). *Artemisia argyi* extract ameliorates IL-17A-induced inflammatory response by regulation of NF-κB and Nrf2 expression in HIG-82 synoviocytes. *Environmental Toxicology, 37*(11), 2793–2803. https://doi.org/10.1002/tox.23637

Commission, C. P.. (2020). *Pharmacopoeia of the People's Republic of China. I*. Beijing: China Medical Science Press.

Cui, Z. H., Li, S. Q., Chang, J. Y., Zang, E. H., Liu, Q., Zhou, B. C., … Li, M. H. (2022). The pharmacophylogenetic relationships of two edible medicinal plants in the genus Artemisia. *Frontiers in Plant Science, 13*. https://doi.org/10.3389/fpls.2022.949743

Du, H., Chen, W. L., Lei, Y. T., Li, F. C., Li, H. M., Deng, W., & Jiang, G. H. (2021). Discrimination of authenticity of Fritillariae *Cirrhosae Bulbus* based on terahertz spectroscopy and chemometric analysis. *Microchemical Journal, 168*, Article 106440. https://doi.org/10.1016/j.microc.2021.106440

Hye Hur, S., Kim, H. Y., Kim, Y. K., An, J. M., Lee, J. H., & Kim, H. J. (2023). Discrimination between Korean and Chinese kimchi using inductively coupled plasma-optical emission spectroscopy and mass spectrometry: A multivariate analysis of kimchi. *Food Chemistry, 423*, Article 136235. https://doi.org/10.1016/j.foodchem.2023.136235

Jeong, S., Seol, D., Kim, H., Lee, Y., Nam, S. H., An, J. M., & Chung, H. (2023). Cooperative combination of LIBS-based elemental analysis and near-infrared molecular fingerprinting for enhanced discrimination of geographical origin of soybean paste. *Food Chemistry, 399*, Article 133956. https://doi.org/10.1016/j.foodchem.2022.133956

Kang, C. D., Zhang, Y. Y., Zhang, M. Y., Qi, J., Zhao, W. T., Gu, J., … Li, Y. Y. (2022). Screening of specific quantitative peptides of beef by LC–MS/MS coupled with OPLS-DA. *Food Chemistry, 387*, Article 132932. https://doi.org/10.1016/j.foodchem.2022.132932

Li, M., Chai, X., Wang, L. Y., Yang, J., & Wang, Y. F. (2019). Study of the variation of phenolic acid and flavonoid content from fresh *Artemisiae argyi* folium to Moxa wool. *Molecules, 24*(24), 4603. https://doi.org/10.3390/molecules24244603

Liu, Y., He, Y. N., Wang, F., Xu, R. C., Yang, M., Ci, Z. M., … Lin, J. Z. (2021). From longevity grass to contemporary soft gold: Explore the chemical constituents, pharmacology, and toxicology of *Artemisia argyi* H.Lév. & vaniot essential oil. *Journal of Ethnopharmacology, 279*, Article 114404. https://doi.org/10.1016/j.jep.2021.114404

Long, Q. Q., Feng, N., Gan, H. X., Zhang, X., Han, Y. P., & Gu, J. (2023). Study on origin traceability of Amur cork-tree bark based on stable isotopes and multielements combined chemometrics. *Industrial Crops and Products, 194*, Article 116380. https://doi.org/10.1016/j.indcrop.2023.116380

Lu, L., Wang, L., Liu, R. Y., Zhang, Y. B., Zheng, X. Q., Lu, J. L., … Ye, J. H. (2024). An efficient artificial intelligence algorithm for predicting the sensory quality of green and black teas based on the key chemical indices. *Food Chemistry, 441*, Article 138341. https://doi.org/10.1016/j.foodchem.2023.138341

Mi, S., Shang, K., Li, X., Zhang, C. H., Liu, J. Q., & Huang, D. Q. (2019). Characterization and discrimination of selected China's domestic pork using an LC-MS-based lipidomics approach. *Food Control, 100*, 305–314. https://doi.org/10.1016/j.foodcont.2019.02.001

Mi, S., Wang, Y. H., Zhang, X. N., Sang, Y. X., & Wang, X. H. (2022). Authentication of the geographical origin of sesame seeds based on proximate composition, multi-element and volatile fingerprinting combined with chemometrics. *Food Chemistry, 397*, Article 133779. https://doi.org/10.1016/j.foodchem.2022.133779

Nie, J., Yang, J., Liu, C. L., Li, C. L., Shao, S. Z., Yao, C. X., … Yuan, Y. W. (2023). Stable isotope and elemental profiles determine geographical origin of saffron from China and Iran. *Food Chemistry, 405*, Article 134733. https://doi.org/10.1016/j.foodchem.2022.134733

Oliveira, M. M., Cruz-Tirado, J. P., & Barbin, D. F. (2019). Nontargeted analytical methods as a powerful tool for the authentication of spices and herbs: A review. *Comprehensive Reviews in Food Science and Food Safety, 18*(3), 670–689. https://doi.org/10.1111/1541-4337.12436

Pacholczyk-Sienicka, B., Modranka, J., & Ciepielowski, G. (2024). Comparative analysis of bioactive compounds in garlic owing to the cultivar and origin. *Food Chemistry, 439*, Article 138141. https://doi.org/10.1016/j.foodchem.2023.138141

Qi, J., Li, Y. Y., Zhang, C., Wang, C., Wang, J. Q., Guo, W. P., & Wang, S. W. (2021). Geographic origin discrimination of pork from different Chinese regions using mineral elements analysis assisted by machine learning techniques. *Food Chemistry, 337*, Article 127779. https://doi.org/10.1016/j.foodchem.2020.127779

Song, X. C., Canellas, E., & Nerin, C. (2021). Screening of volatile decay markers of minced pork by headspace-solid phase microextraction–gas chromatography–mass spectrometry and chemometrics. *Food Chemistry, 342*, Article 128341. https://doi.org/10.1016/j.foodchem.2020.128341

Song, X. W., Wen, X., He, J. W., Zhao, H., Li, S. M., & Wang, M. Y. (2019). Phytochemical components and biological activities of *Artemisia argyi*. *Journal of Functional Foods, 52*, 648–662. https://doi.org/10.1016/j.jff.2018.11.029

Su, S. H., Sundhar, N., Kuo, W. W., Lai, S. C., Kuo, C. H., Ho, T. J., … Huang, C. Y. (2022). *Artemisia argyi* extract induces apoptosis in human gemcitabine-resistant lung cancer cells *via* the PI3K/MAPK signaling pathway. *Journal of Ethnopharmacology, 299*, Article 115658. https://doi.org/10.1016/j.jep.2022.115658

Wang, H. B., Zhang, M. L., Ma, Y. R., Wang, B., Shao, M. W., Huang, H., … Kang, Z. H. (2020). Selective inactivation of gram-negative bacteria by carbon dots derived from natural biomass: *Artemisia argyi* leaves. *Journal of Materials Chemistry B, 8*(13), 2666–2672. https://doi.org/10.1039/C9TB02735A

Wang, Z. C., Wang, L., Huang, H. T., Li, Q. Y., Wang, X. Y., Sun, Q., … Li, N. (2023). *In vitro* antioxidant analysis of flavonoids extracted from *Artemisia argyi* stem and their anti-inflammatory activity in lipopolysaccharide-stimulated RAW 264.7 macrophages. *Food Chemistry, 407*, Article 135198. https://doi.org/10.1016/j.foodchem.2022.135198

Wei, J., Wang, Y., Tang, X., Du, Y., Bai, Y., Deng, Y., … Kang, J. (2024). Correlation analysis between active components of *Cornus officinalis* and inorganic elements in rhizosphere soil and rapid analysis of origin quality by near-infrared spectroscopy combined with machine learning. *Industrial Crops and Products, 210*, Article 118101. https://doi.org/10.1016/j.indcrop.2024.118101

Wu, F. H., Zhao, H. A., Sun, J., Guo, J. B., Wu, L. M., Xue, X. F., & Cao, W. (2021). ICP-MS-based ionomics method for discriminating the geographical origin of honey of *Apis cerana* Fabricius. *Food Chemistry, 354*, Article 129568. https://doi.org/10.1016/j.foodchem.2021.129568

Wu, L. K., Agarwal, S., Kuo, C. H., Kung, Y. L., Day, C. H., Lin, P. Y., … Chiang, C. Y. (2022). Artemisia leaf extract protects against neuron toxicity by TRPML1 activation and promoting autophagy/mitophagy clearance in both *in vitro* and *in vivo* models of MPP+/MPTP-induced Parkinson's disease. *Phytomedicine, 104*, Article 154250. https://doi.org/10.1016/j.phymed.2022.154250

Wu, W., Xiang, F., & He, F. (2021). Polyphenols from *Artemisia argyi* leaves: Environmentally friendly extraction under high hydrostatic pressure and biological activities. *Industrial Crops and Products, 171*, Article 113951. https://doi.org/10.1016/j.indcrop.2021.113951

Xiao, J. Q., Liu, W. Y., Sun, H. P., Li, W., Koike, K., Kikuchi, T., … Zhang, J. (2019). Bioactivity-based analysis and chemical characterization of hypoglycemic and antioxidant components from *Artemisia argyi*. *Bioorganic Chemistry, 92*, Article 103268. https://doi.org/10.1016/j.bioorg.2019.103268

Ye, Y. Y., Yan, W., Peng, L. J., He, J. L., Zhang, N., Zhou, J. J., … Cai, J. (2023). Minerals and bioactive components profiling in se-enriched green tea and the Pearson correlation with se. *LWT, 175*, Article 114470. https://doi.org/10.1016/j.lwt.2023.114470

Yoon, D., Shin, W. C., Oh, S. M., Choi, B. R., & Young Lee, D. (2022). Integration of multiplatform metabolomics and multivariate analysis for geographical origin discrimination of *Panax ginseng*. *Food Research International, 159*, Article 111610. https://doi.org/10.1016/j.foodres.2022.111610

Yu, D. X., Guo, S., Zhang, X., Yan, H., Mao, S. W., Wang, J. M., … Duan, J. A. (2023). Combining stable isotope, multielement and untargeted metabolomics with chemometrics to discriminate the geographical origins of ginger (*Zingiber officinale* roscoe). *Food Chemistry, 426*, Article 136577. https://doi.org/10.1016/j.foodchem.2023.136577

Zhan, H., Xu, W. F., Zhao, X. X., Tian, L. L., Zhang, F., Wei, H., & Tao, X. Y. (2022). Effects of Lactiplantibacillus plantarum WLPL01 fermentation on antioxidant activities, bioactive compounds, and flavor profile of *Artemisia argyi*. *Food Bioscience, 49*, Article 101908. https://doi.org/10.1016/j.fbio.2022.101908

Zhang, D., Yao, L. M., Chang, Y. Q., Yang, G. Y., Xue, Z. J., Wang, L., … Guo, L. (2021). Evaluation and comparison of bioactive constituents of *Artemisiae argyi* folium collected at different developmental stages. *Journal of AOAC International, 104*(2), 515–525. https://doi.org/10.1093/jaoacint/qsaa105

Zhang, H. R., Liu, W. Y., Shen, Q. S., Zhao, L. Y., Zhang, C. H., & Richel, A. (2021). Discrimination of geographical origin and species of China's cattle bones based on multi-element analyses by inductively coupled plasma mass spectrometry. *Food Chemistry, 356*, Article 129619. https://doi.org/10.1016/j.foodchem.2021.129619

Zhang, X. W., Wang, S., Tu, P. F., & Zeng, K. W. (2018). Sesquiterpene lactone from *Artemisia argyi* induces gastric carcinoma cell apoptosis *via* activating NADPH oxidase/reactive oxygen species/mitochondrial pathway. *European Journal of Pharmacology, 837*, 164–170. https://doi.org/10.1016/j.ejphar.2018.07.053